193. 8-Aza-7-deazaadenine N^8- and N^9-(β-D-2′-Deoxyribofuranosides): Building Blocks for Automated DNA Synthesis and Properties of Oligodeoxyribonucleotides

by **Frank Seela*** and **Klaus Kaiser**

Laboratorium für Organische und Bioorganische Chemie, Fachbereich Biologie/Chemie, Universität Osnabrück, Barbarastrasse 7, D-4500 Osnabrück

(18.VIII.88)

Oligonucleotides with alternating 8-aza-7-deaza-2′-deoxyadenosine (= $c^7z^8A_d$ **2**) and dT residues (see **11**, **14** and **16**) or 4-aminopyrazolo[3,4-*d*]pyrimidine N^2-(β-D-2′-deoxyribofuranoside) (= $c^7z^8A'_d{}^1$); **3**) and dT residues (see **12**) have been prepared by solid-phase synthesis using P(III) chemistry. Additionally, palindromic oligomers derived from d(C-T-G-G-A-T-C-C-A-G) but containing **2** or **3** instead of dA (see **18**–**22**) have been synthesized. Benzoylation of **2** or **3**, followed by 4,4′-dimethoxytritylation and subsequent phosphitylation yielded the methyl or the cyanoethyl phosphoramidites **8a**,**b** and **9**. They were employed in automated DNA synthesis. Alternating oligomers containing **2** or **3** showed increase dT_m values compared to those with dA, in particular **12** with an unusual N^2-glycosylic bond. The palindromic oligomers **18**–**22** containing **2** or **3** instead of dA were used as sequence-specific probes in endonuclease Sau 3A phosphodiester hydrolysis. Whereas replacement of dA outside of the enzymic recognition side reduced the hydrolysis rate, replacement within d(G-A-T-C) abolished phosphodiester hydrolysis.

Introduction. – DNA can adopt several forms of tertiary structure [1]. This depends on the hydratization of the molecule, on the binding of small ions, or on the interaction with high-molecular-weight proteins. Moreover, the tertiary structure is controlled by the sequence. Alternating d(G-C) regions can induce B–Z transitions [2] or a bending takes place if d(C-A_{5-6}-T) tracts are found as repeating units [3].

Currently, our laboratory has reported on the synthesis of pyrazolo[3,4-*d*]pyrimidine N^1- and N^2-(β-D-2′-deoxyribofuranosides) [4]. These compounds are formed by phase-transfer glycosylation of pyrazolo[3,4-*d*]pyrimidines. The compounds with a N^1-glycosylic bond (see *e.g.* **2**) are isosteric to the parent purine nucleosides (see **1**), whereas the N^2 regioisomers (see *e.g.* **3**) have no counterpart in nature.

Inspection of CPK models shows that pyrazolo[3,4-*d*]pyrimidine N^1- as well as N^2-nucleosides should form *Watson-Crick* base-paired duplexes, but with an altered tertiary structure in the case of an N^2-deoxyribofuranoside. Therefore, we considered the incorporation of **2** or **3** into alternating or palindromic oligonucleotides. The latter belong to oligomers with the recognition sequence d(G-A-T-C) of the endodeoxyribonuclease Sau 3A [5], but containing **2** or **3** in place of dA. The oligomers were studied with respect to duplex stability or regiospecific enzymic hydrolysis.

Results and Discussion. – In order to incorporate compounds **2** or **3** into oligonucleotides by P(III) chemistry [6], suitable building blocks had to be prepared. This required the choice of the most appropriate protecting groups and the preparation of phosphoramidites which can be directly used in automated solid-phase synthesis. The nucleosides **2**

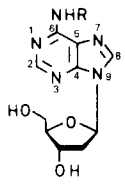

1a R = H (purine numbering)
b R = Bz

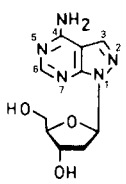

2 (systematic numbering)

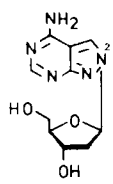

3

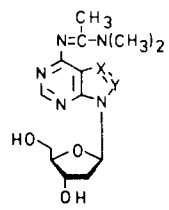

6a X = N, Y = CH
b X = CH, Y = N

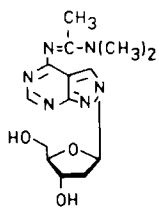

7

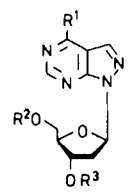

4a $R^1 = OCH_3$, $R^2 = R^3$ = Tol
b R^1 = NHBz, $R^2 = R^3 = H$
c R^1 = NHBz, $R^2 = (MeO)_2Tr$, $R^3 = H$

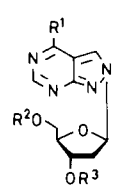

5a $R^1 = OCH_3$, $R^2 = R^3$ = Tol
b R^1 = NHBz, $R^2 = R^3 = H$
c R^1 = NHBz, $R^2 = (MeO)_2Tr$, $R^3 = H$

or **3** have been obtained earlier by liquid-liquid phase-transfer glycosylation [4]. We have now employed the solid-liquid technique [7] being superior to the former method.

The glycosylation of 4-methoxy-1*H*-pyrazolo[3,4-*d*]pyrimidine [8] with 2-deoxy-3,5-di-*O*-(*p*-toluoyl)-α-D-*erythro*-pentofuranosyl chloride [9] was carried out in MeCN with an excess of powdered KOH. This reaction proceeded already in the absence of a phase-transfer catalyst and was complete after 25 min at room temperature. Crystalline **4a** (47%) and **5a** (28%), apart from 7% of 1-[2′-deoxy-3′,5′-di-*O*-(*p*-toluoyl)-α-D-*erythro*-pentofuranosyl]-4-methoxy-1*H*-pyrazolo[3,4-*d*]pyrimidine [4], were obtained. Compared to liquid-liquid conditions, the amount of β-D-nucleosides were increased ([4]: **4a**, 39%; **5a**, 18%).

Removal of the toluoyl groups from **4a** or **5a** was accomplished in NH_3/MeOH resulting in a simultaneous displacement of the 4-MeO group by NH_2. The nucleoside **2** was isolated crystalline in 85%, compound **3** was formed in 92% yield. For 4-NH_2-protection of **2** or **3**, the benzoyl (bz) group was chosen being already successfully used in case of dA. The sugar OH groups were temporarily protected by trimethylsilyl residues (transient protection) [10]. Compound **4b** was isolated in 75% yield; similarly, compound **5b** was obtained in 85%.

Alternatively to benzoylation, **2** or **3** were converted into the methylamidines **6b** or **7** (Me_2N–C(Me)=: m_2ma). This method circumvented intermediate protection of the sugar OH groups and followed a protocol already described for regular nucleosides [11]. Compound **6b** was isolated in 75% yield, whereas **7** was formed in 60%. Structural proof was made by ^{1}H- and ^{13}C-NMR spectroscopy *(Table 1)*. The ^{1}H-NMR spectra of **6b** and **7** showed only one signal for the Me_2N groups at 298 K. This signal was broadened with decreasing temperature and separated into two signals at lower temperature. A coalescence at 296 K was found for **6b** and at 287 K for **7** indicating the differences in the height of the rotation barrier. Apart from the methylamidines, we have tried to synthesize H-amidines by reaction of **2** or **3** with dimethylformamide dimethyl acetal. Unfortu-

Table 1. *^{13}C-NMR Chemical Shifts* ($(D_6)Me_2SO$) *of 2′-Deoxyribofuranosyl Derivatives of Pyrazolo[3,4-d]pyrimidines*[a])

	C(3)	C(3a)	C(4)	C(6)	C(7a)	CH_3O	CH_3–*C*	*C*H_3–C	CH_3N	C=O	C(1′)	C(2′)	C(3′)	C(4′)	C(5′)
2 [4]	132.8	100.4	157.3	155.7	153.6	–	–	–	–	–	84.1	38.0	71.0	87.5	62.3
4b	132.7	104.3	154.6	154.4	152.5	–	–	–	–	166.2	83.8	38.5	70.8	87.5	62.2
4c	132.5	104.3	154.6	154.3	152.5	54.7	–	–	–	166.5	83.7	38.5	70.8	85.3	64.1
3 [4]	132.6	101.3	159.4	156.6	159.5	–	–	–	–	–	90.5	40.3	70.6	88.3	62.0
5b	128.8	104.0	–	155.0	–	–	–	–	–	–	88.7	40.3	70.6	91.0	62.0
5c	126.5	113.1	157.9	155.0	158.0	54.9	–	–	–	–	85.4	40.3	70.4	86.5	63.9
6b	133.7	108.3	162.1	155.7	154.3	–	163.0	17.0	38.1	–	84.2	38.6	71.2	87.7	62.6
7	124.6	108.6	162.8	156.4	160.4	–	164.0	16.9	37.9	–	88.5	38.3	70.5	90.8	61.8

[a]) δ Values given in ppm relative to Me_4Si as internal standard.

Table 2. *Half-Life Values* ($\tau/2$) *of Deprotection of Pyrazolo[3,4-d]pyrimidine 2′-Deoxyribonucleosides*[a])

Compd.		$\tau/2$ [min]	
		25% aq. NH_3	0.2N NaOH/MeOH 1:1
bz^6A_d	(**1b**) [10]	170[b])	67[b])
$bz^6c^7z^8A_d$	(**4b**)	525[b])	25[b])
$bz^6c^7z^8A'_d$[1])	(**5b**)	290[c])	17[c])
$m_2ma^6A_d$	(**6a**) [11]	500[d])	580[d])[e])
$m_2ma^6c^7z^8A_d$	(**6b**)	15[f])	158[f])
$m_2ma^6c^7z^8A'_d$[1])	(**7**)	8[c])	92[c])

[a]) At 20 μM nucleoside concentration and 40°.
[b]) Measured UV-spectrophotometrically at 295 nm.
[c]) See *Footnote b*, at 319 nm.
[d]) See *Footnote b*, at 315 nm.
[e]) At 60°.
[f]) See *Footnote b*, at 312 nm.

nately, the H-amidines were too labile and were deprotected during the workup procedure. This is analogous to the situation with dA [12] but different to the one with 7-deaza-2′-deoxyadenosine [13].

As the 4-NH_2 protecting groups of **2** and **3** had to be stable during oligonucleotide synthesis but removable under alkaline conditions, we have carried out hydrolysis experiments in conc. aq. NH_3 solution and in 0.2N NaOH/MeOH 1:1. TLC monitoring confirmed that deprotection gave back the nucleosides **2** or **3** as the only products. No by-products were detected. From *Table 2* it is apparent that the benzoylated compounds **4b** or **5b** were less easily hydrolyzed in conc. NH_3 than the amidines **6b** or **7** and that the hydrolysis rate of the N^2 compounds was enhanced compared to the N^1 isomers. This is opposite to the situation with the corresponding purines. However, when the reaction was carried out in 0.2N NaOH/MeOH 1:1, the amidines **6b** or **7** were more stable than the benzoylated compounds **4b** or **5b** which is in line with the corresponding purines **1b** and **6a**. The differences of $\tau/2$ values between aq. NH_3 solution and 0.2N NaOH/MeOH 1:1 may be due to a change of the reaction mechanism[2]) and/or differences in solvation. As

[1]) A'_d is the symbol used for the 2′-deoxyadenosine moiety with the unusual N^8- instead of the usual N^9-glycosidic linkage (purine numbering, see **1**). The group Me_2N–C(Me)= is represented by m_2ma.

[2]) The differences can also be attributed to the different attacking nucleophile (NH_3 *vs.* OH^-).

NH_3 is commonly employed upon deprotection of oligonucleotides in which the amidines are rather labile, the benzoylated compounds **4b** and **5b** were used for further experiments.

The 4,4′-dimethoxytrityl ($(MeO)_2Tr$) residue [14] was chosen as 5′-protecting group for compounds **4b** and **5b**. This was accomplished in pyridine with an excess of 4,4′-dimethoxytrityl chloride in the presence of 4-(dimethylamino)pyridine. Compounds **4c** or **5c** were purified by flash chromatography and isolated as amorphous foams. The downfield shift of C(5′) and an upfield location of C(4′) confirmed 5′-protection *(Table 1)*.

Phosphitylation [17] of **4c** or **5c** with chloro(diisopropylamino)methoxyphosphine in CH_2Cl_2 in the presence of $(i\text{-}Pr)_2EtN$ yielded the phosphoramidites **8a** and **9**. The phosphoramidite **8b** was prepared in a similar way by using chloro(2-cyanoethoxy)-(diisopropylamino)phosphine [16]. Purification of the phosphoramidites was accomplished by flash chromatography resulting in colorless solids which were characterized by ^{31}P-NMR spectroscopy.

The synthesis of the oligonucleotides **10**–**22** was carried out on solid support [15] in an automated DNA synthesizer using the regular phosphoramidites of dA, dT, dC, and dG [17] and the modified phosphoramidites **8a**/**b** or **9**. The synthesis followed a protocol of detritylation, coupling, capping, and oxidation according to [18]. The protected oligomers were demethylated with thiophenol and cleaved from solid support by brief treatment with NH_3. After removal of the base-protecting groups by ammonolysis, purification of the $(MeO)_2Tr$-protected oligomers by reverse-phase HPLC, and removal of the $(MeO)_2Tr$ residue with 80% aqueous AcOH (see *Exper. Part*), the oligomers **10**–**22** were recovered. They were purified by reverse-phase HPLC and obtained as colorless solids upon lyophilization.

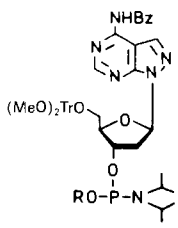

8a R = CH_3
b R = $(CH_2)_2CN$

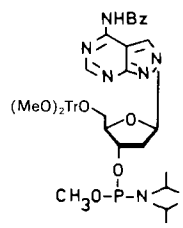

9

d(A-T)$_6$ **10** d(c^{7}z^{8}A-T)$_6$ **11** d(c^{7}z^{8}A′-T)$_6$ **12**[1])

d(A-T)$_9$ **13** d(c^{7}z^{8}A-T)$_9$ **14** d(A-T)$_{12}$ **15** d(c^{7}z^{8}A-T)$_{12}$ **16**

d(C-T-G-G-A-T-C-C-A-G) **17** d(C-T-G-G-c^{7}z^{8}A-T-C-C-c^{7}z^{8}A-G) **18**

d(C-T-G-G-c^{7}z^{8}A-T-C-C-A-G) **19** d(C-T-G-G-A-T-C-C-c^{7}z^{8}A-G) **20**

d(C-T-G-G-c^{7}z^{8}A′-T-C-C-A-G) **21** d(C-T-G-G-A-T-C-C-c^{7}z^{8}A′-G) **22**[1])

The nucleoside content of **10**–**22** was determined after tandem hydrolysis with snake-venom phosphodiesterase and alkaline phosphatase. Reverse-phase HPLC of the hydrolysis mixture separated the nucleosides. Quantitative UV spectrophotometry, using the extinction coefficients of the monomers confirmed the molar content of the monomers and showed that no side-reaction had occurred during oligonucleotide synthesis.

Melting Profiles of the Oligomers 10–16. – The sigmoidal melting profiles of the oligonucleotides **10**–**16** (conditions, see *Exper. Part* or *Table 3*) confirmed cooperative helix-coil transitions in all cases. The T_m values are listed in *Table 3*. As can be seen, the

Table 3. *Melting Temperatures* (T_m Values) *of the Oligonucleotides* **10–12**[a]), **13–16**[b]), *and* **17–22**[c])

Oligomer		T_m [°]	Oligomer		T_m [°]
d(A-T)	(**10**)	32[d])	d(C-T-G-G-A-T-C-C-A-G)	(**17**)	48
$d(c^7z^8A\text{-}T)_6$	(**11**)	36	d(C-T-G-G-c^7z^8A-T-C-C-c^7z^8A-G)	(**18**)	47
$d(c^7z^8A'\text{-}T)_6$[l])	(**12**)	48	d(C-T-G-G-c^7z^8A-T-C-C-A-G)	(**19**)	47
$d(A\text{-}T)_9$	(**13**)	51	d(C-T-G-G-A-T-C-C-c^7z^8A-G)	(**20**)	46
$d(c^7z^8A\text{-}T)_9$	(**14**)	54	d(C-T-G-G-c^7z^8A′-T-C-C-A-G)[l])	(**21**)	35
$d(A\text{-}T)_{12}$	(**15**)	59	d(C-T-G-G-A-T-C-C-c^7z^8A′-G)[l])	(**22**)	45
$d(c^7z^8A\text{-}T)_{12}$	(**16**)	63			

[a]) In 1M NaCl, 0.1M $MgCl_2$, and 60 mM cacodylic acid, pH 7.0, at 6 μM single-strand concentration.
[b]) In 1M NaCl, 0.1M $MgCl_2$, and 60 mM cacodylic acid, pH 7.0 at 3 μM single-strand concentration.
[c]) In 20 mM *Tris*-HCl buffer pH 8.5 containing 10 mM $MgCl_2$, at 4 μM single-strand concentration.
[d]) Values were determined at 260 nm with 1° error limit.

oligomers containing 8-aza-7-deazaadenine exhibit definitely higher T_m values than those with adenine. Surprisingly, the oligonucleotide **12**, containing the N^2-nucleoside **3** instead of **2** showed a T_m value which was 12° higher compared to that of **11** and 16° compared to the unmodified oligomer **10**.

In order to get more information about duplex stability, concentration-depending melting experiments were carried out. This allowed the determination of thermodynamic parameters of helix-coil transition. The oligomer concentration was varied between 3 and 80 μM. *Fig. 1* shows the plot of the $1/T_m$ values *vs.* log of concentration. The ΔG, ΔH, and ΔS values were calculated according to [19] assuming a two-state model for helix formation. As can be seen from *Table 4*, the enthalpy values correspond to the melting temperatures. Good agreement is also found for the thermodynamic values of the oligomer **10** with data published by *Wilson* and coworkers [20].

The increase of T_m values of oligonucleotides containing 8-aza-7-deazaadenine in place of adenine can be explained by the following: Oligomer d(A–T) forms a special type

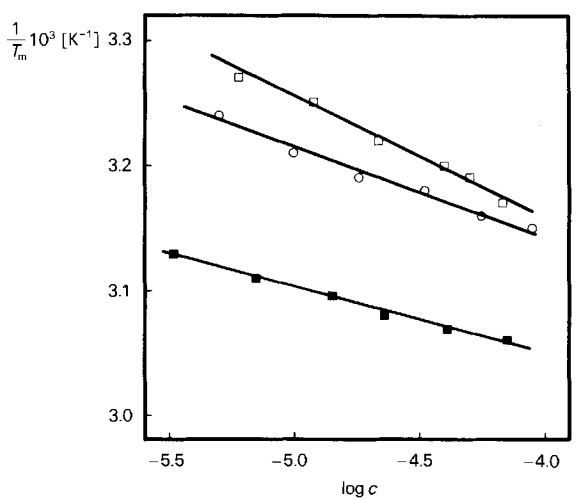

Fig. 1. *Plot of* $1/T_m$ vs. *log concentration of the oligomers* **10** (□), **11** (○), *and* **12** (■) *in* H_2O. All solutions contain 1.0M NaCl, 0.1M $MgCl_2$, and 60 mM sodium cacodylate, pH 7.0.

Table 4. *Thermodynamic Parameters for Helix Formation of the Dodecamers* **10–12**

Dodecamer		ΔH [kcal/mol]	ΔS [cal/mol·K]	ΔG [kcal/mol][a])	T_m [°][b])
d(A-T)$_6$	(**10**)	–47	–130	–6.7	32
d(c^{7}z^{8}A-T)$_6$	(**11**)	–63	–180	–7.2	36
d(c^{7}z^{8}A′-T)$_6$[1])	(**12**)	–87	–245	–11.0	48

[a]) Calculated at 37°. [b]) Dodecamer concentration was 6 μM.

of a DNA duplex with a poor base overlap [21]. As a result, the lac repressor protein binds about 1000-fold more tightly to poly[d(A–T)]·poly[d(A–T)] than to calf thymus DNA [22]. The poor overlap between purine and pyrimidine bases results in weaker stacking interactions as found within a random arrangement. The different π-electron distribution of 8-aza-7-deazaadenine compared to adenine which results in altered dipole moments changes this behavior resulting in a probably stronger stacking interaction.

Regarding the extraordinary high T_m value of the oligonucleotide **12** containing the N^2-glycoside compared to **11** or **10**, a special tertiary structure has to be discussed. From CPK-model building, it becomes apparent that duplex formation by *Watson-Crick* base-pairing causes differences of helical parameters, *e.g.* the height of the helix pitch and a change of the sugar puckering. According to the N^2-glycosylic bond of **3**, the electron distribution of the nucleobase is also affected. This may influence H-bonding which is important in duplex stabilization. The extraordinary stability of **12** needs further investigation by other techniques such as X-ray spectroscopy or two-dimensional NMR.

Endodeoxyribonuclease Sau 3A Phosphodiester Hydrolysis of Oligonucleotides Containing Compounds 2 or 3. – The endodeoxyribonuclease Sau 3A binds to the duplex d(G-A-T-C)·d(G-A-T-C) and hydrolyses the phosphodiester bond between dG and the 5′-neighboured nucleotide [5]. As compound **2** is one of the most similar structural analogues of dA (**1a**), we have synthesized the oligomers **18–20** (see above) in which dA is

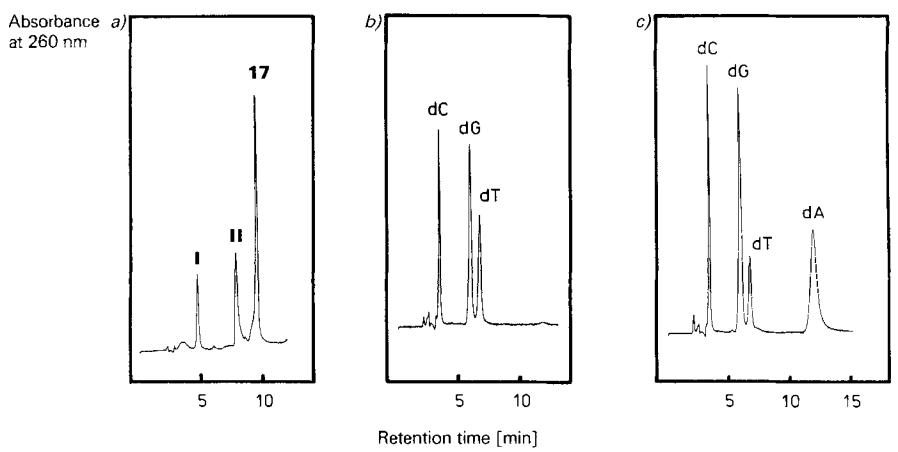

Fig. 2. *HPLC profiles from the hydrolysis of d(C-T-G-G-A-T-C-C-A-G)* (**17**) *by the endodeoxyribonuclease Sau 3A under the conditions described in the* Exper. Part. *a)* HPLC profile of the reaction mixture, solvent *II*; *b) c)* HPLC patterns of the cleavage products d(C-T-G) (**I**) and d(pG-A-T-C-C-A-G) (**II**), respectively, after cleavage with snake-venom phosphodiesterase and treatment with alkaline phosphatase, solvent III.

replaced by $c^7z^8A_d$ (**2**) at various positions; either within the recognition sequence or in its flanking region. We have also prepared **21** and **22** to study enzymic hydrolysis at oligomers containing $c^7z^8A'_d{}^1$) (**3**) in place of dA.

Fig. 2 shows that the oligomer **17** is cleaved into the fragments d(C-T-G) (**I**) and d(pG-A-T-C-C-A-G) (**II**). The cleavage experiments were carried out at 25° which ensured duplex formation under hydrolysis conditions. The hydrolysis products were identified by tandem hydrolysis with snake-venom phosphodiesterase followed by alkaline phosphatase and separation by HPLC *(Fig. 2)*. Under the same conditions, the hydrolysis of the decamers **18**–**22** was investigated. The experiments with **18**, **19**, or **21** showed that replacement of both dA by **2** or **3** leads to complete disappearance of hydrolysis *(Fig. 3)*. On the other hand, replacement of one dA residue outside of the enzymic recognition site by **2** or **3** reduced only the hydrolysis rate (see **20** and **22** in *Fig. 3*). This demonstrates that dA within the sequence d(G-A-T-C) is specifically recognized by the enzyme.

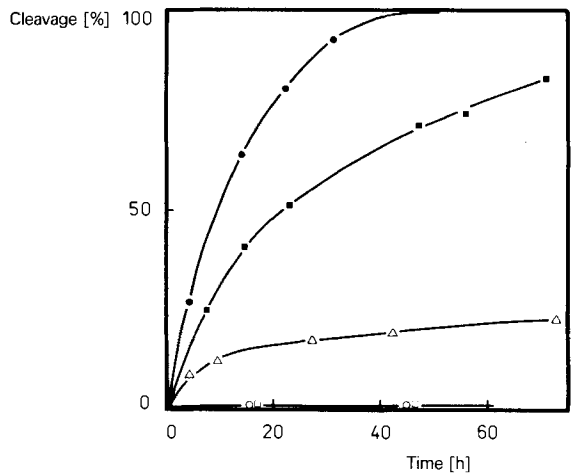

Fig. 3. *Time course of phosphodiester hydrolysis of the oligomers d(C-T-G-G-A-T-C-C-A-G)* (**17**, ●), *d(C-T-G-G-c^7z^8A-T-C-C-c^7z^8A-G)* (**18**, ○), *d(C-T-G-G-c^7z^8A-T-C-C-A-G)* (**19**, □), *d(C-T-G-G-A-T-C-C-c^7z^8A-G)* (**20**, ■), *and d(C-T-G-G-A-T-C-C-c^7z^8A'-G)*^{1}) (**22**, △) *by treatment with the endodeoxyribonuclease Sau 3A*. Conditions, see *Exper. Part.*

The results obtained with the 8-aza-7-deazapurine N^1-nucleoside **2** are different to those obtained by *Ueda* and coworkers [23] replacing dA by the 7-deazapurine nucleoside 2′-deoxytubercidin (c^7A_d) within the oligomer d(pG-G-A-*G-A-T-C*-T-C-C). In that case, the endodeoxyribonuclease Sau 3A hydrolysis rate was only reduced if c^7A_d substituted dA within the recognition site but was not touched at all if c^7A_d was incorporated into the flanking regions. A dA/c^7A_d replacement within the recognition sequence d(G-T-A-*G-c^7A-A-T-T-C*-T-A-C) of the endodeoxyribonuclease Eco RI was recently carried out in our laboratory and gave similar results [24]. As it has been shown [25] that dA within the Eco RI recognition site is bound to the enzyme *via* NH_2–C(6) and N(7), we consider the same interaction in case of the endodeoxyribonuclease Sau 3A with its cognate DNA fragment d(G-A-T-C). Apparently, endodeoxynucleases are able to accommodate a partial loss of binding sites still exhibiting slow but regiospecific phosphodiester hydro-

lysis. The reason for the complete disappearance of hydrolysis in case of **18**, **19**, and **21** may be due to the loss of the purine N(7) binding site as well as to tertiary structure changes caused by 8-aza-7-deazaadenine which seems to be less severe in case of 7-deazaadenine.

According to *Table 3*, the melting temperatures of the oligomers **17–20** and **22** are almost identical. However, a strong destabilization is observed in case of the duplex of **21**, in which two of the N(2)-linked nucleosides **3** are centred in the middle of the oligomer. At that location, it brings discontinuity into the helix. This is different to the oligomer **12** which can form a new uniform helix being even more stable than corresponding duplexes with regularly linked nucleosides.

Financial support by the *Deutsche Forschungsgemeinschaft* and the *Stiftung Volkswagenwerk* is gratefully acknowledged.

Experimental Part

General. See [26]. The protected phosphoramidites were synthesized according to the procedure of *McBride* and *Caruthers* [17] and *Sinha et al.* [16]. *Fractosil 500* polymeric support was purchased from *Biosyntech* (Hamburg, FRG). Oligonucleotide synthesis was carried out on an automated DNA synthesizer, model *380 B*, of *Applied Biosystems* (Weiterstadt, FRG). Endodeoxyribonuclease Sau 3A, alkaline phosphatase (EC 3.1.3.1), and snake-venom phosphodiesterase (EC 3.1.16.1) were purchased from *Boehringer* (Mannheim, FRG). Flash chromatography (FC): 0.5 bar, silica gel *60H* (*Merck*, FRG); solvent systems: CH_2Cl_2/AcOEt 95:5 (*A*), CH_2Cl_2/AcOEt 9:1 (*B*), CH_2Cl_2/MeOH 8:2 (*C*), $CHCl_3$/MeOH 9:1 (*D*), CH_2Cl_2/acetone 9:1 (*E*), CH_2Cl_2/acetone 8:2 (*F*), CH_2Cl_2/acetone 6:4 (*G*), CH_2Cl_2/MeOH 9:1 (*H*), CH_2Cl_2/acetone 7:3 (*I*), CH_2Cl_2/AcOEt/Et_3N 75:25:5 (*K*), and CH_2Cl_2/AcOEt 1:1 (*L*). Reverse-phase HPLC: Solvent systems containing 0.1M Et_3NHOAc of pH 7.0 (*A*) and MeCN (*B*) were used system *I*, 25–40% *B* in *A* for 10 min; system *II*, 10–25% *B* in *A* for 10 min; system *III*, 5% *B* in *A*; flow rates for *I–III*: 1 ml/min.

*Solid-Liquid Phase-Transfer Glycosylation of 4-Methoxy-1*H*-pyrazolo[3,4-*d*]pyrimidine with 2-Deoxy-3,5-di-*O*-(*p*-toluoyl)-α-*D*-erythro-pentofuranosyl Chloride.* Powdered KOH (336 mg, 6 mmol) and 4-methoxy-1*H*-pyrazolo[3,4-*d*]pyrimidine [8] (180 mg, 1.4 mmol) were stirred at r.t. in anh. MeCN (50 ml). After 15 min, 2-deoxy-3,5-di(*p*-toluoyl)-α-*D*-*erythro*-pentofuranosyl chloride [9] (530 mg, 1.3 mmol) was added. Stirring was continued for 10 min, unsoluble material removed by filtration and washed with MeCN, the filtrate evaporated to dryness, and the residue submitted to FC on a silica gel *60H* column (15 × 4 cm).

*1-[2'-Deoxy-3',5'-di-*O*-(p-toluoyl)-β-D-*erythro*-pentofuranosyl]-4-methoxy-1*H*-pyrazolo[3,4-d]pyrimidine* (**4a**). FC: from the fast migrating zone (eluant *A*), **4a** was isolated as a colorless foam (280 mg, 47%). Crystallization from i-PrOH afforded colorless needles. M.p. 95° ([4]: 95–98°).

*1-[2'-Deoxy-3',5'-di-*O*-(p-toluoyl)-α-D-*erythro*-pentofuranosyl]-4-methoxy-1*H*-pyrazolo[3,4-d]pyrimidine.* FC: from the 2nd zone, colorless amorphous 1-[2'-deoxy-3',5'-di-*O*-(*p*-toluoyl)-α-*D*-*erythro*-pentofuranosyl]-4-methoxy-1*H*-pyrazolo[3,4-*d*]pyrimidine (40 mg, 7%) was obtained. UV (MeOH): 241 ([4]: 241).

*2-[2'-Deoxy-3',5'-di-*O*-(p-toluoyl)-β-D-*erythro*-pentofuranosyl]-4-methoxy-2*H*-pyrazolo[3,4-d]pyrimidine* (**5a**). FC: the slow migrating zone (eluted with *B*) yielded colorless foamy **5a** (165 mg, 27.5%) upon evaporation. Crystallization from i-PrOH gave colorless crystals. M.p. 164° ([4]: 162–164°).

*4-Amino-1-(2'-deoxy-β-D-*erythro*-pentofuranosyl)-1*H*-pyrazolo[3,4-d]pyrimidine* (**2**). Compd. **4a** (3 g, 6 mmol) in MeOH (80 ml, saturated with NH_3 at 0°) was stirred for 48 h at 60°. The soln. was evaporated, the residue adsorbed on silica gel *60H* (10 g) and applied to the top of a silica gel *60H* column (20 × 2.5 cm). After FC (*C*), **2** (1.3 g, 86%) was obtained as a colorless foam which crystallized from i-PrOH. M.p. 245° ([4]: 245–246°).

*4-Amino-2-(2'-deoxy-β-D-*erythro*-pentofuranosyl)-2*H*-pyrazolo[3,4-d]pyrimidine* (**3**). A soln. of **5a** (1.5 g, 3 mmol) in MeOH (50 ml, saturated with NH_3 at 0°) was stirred for 48 h at 60°. Workup identical with that of **2** yielded **3** as a colorless solid (700 mg, 92%) which crystallized from EtOH/pentane. M.p. 198° ([4]: 197–200°).

*4-(Benzoylamino)-1-(2'-deoxy-β-D-*erythro*-pentofuranosyl)-1*H*-pyrazolo[3,4-d]pyrimidine* (**4b**). Compd. **2** (700 mg, 2.8 mmol) was dried by co-evaporation with anh. pyridine and then dissolved in pyridine (10 ml). Me_3SiCl (3.7 ml, 28 mmol) was added, the soln. stirred for another 2 h, treated with benzoyl chloride (400 µl, 3.1 mmol), and maintained at r.t. for 2 h. The mixture was cooled (ice bath) and diluted with H_2O (4 ml). After 5 min, the resultant was treated with 25% aq. NH_3 (5 ml) for 30 min and evaporated. The residue was dissolved in H_2O (50 ml) and **4b** crystallized from a reduced volume as colorless needles (750 mg, 75%). TLC (silica gel, *D*): R_f 0.45. UV (MeOH):

240 (16400), 275 (15200), 285 (14400). M.p. 184–185°. ^{1}H-NMR ((D$_6$)DMSO): 2.33 (*m*, H$_b$–C(2′)); 2.85 (*m*, H$_a$–C(2′)); 3.51 (*m*, H–C(5′)); 3.84 (*m*, H–C(4′)); 4.48 (*m*, H–C(3′)); 4.74 (*t*, *J* = 6, OH–C(5′)); 5.32 (*d*, *J* = 4, OH–C(3′)); 6.75 (*dd*, *J* = 6, H–C(1′)); 7.53–8.11 (*m*, arom. H); 8.48 (*s*, H–C(3)); 8.77 (*s*, H–C(6)); 11.39 (*s*, NH). Anal. calc. for $C_{17}H_{17}N_5O_4$: C 57.47, H 4.82, N 19.71; found: C 57.36, H 4.95, N 19.83.

*1-(2′-Deoxy-β-*D-erythro-*pentofuranosyl)-4-{[1-(dimethylamino)ethylidene]amino}-1*H-*pyrazolo[3,4-*d*]pyrimidine* (**6b**). Compd. **2** (300 mg, 1.2 mmol) was coevaporated 2 times with anh. pyridine and then dissolved in MeOH (10 ml). *N,N*-Dimethylacetamide dimethyl acetal (0.5 ml, 3 mmol) was added and the soln. stirred at 40° for 8 h. MeOH was removed by co-evaporation and the residue applied to a 10 × 2.5-cm silica gel *60H* column. FC (*H*) yielded **6b** (300 mg, 78%) as a colorless foam. TLC (silica gel, *H*): R_f 0.4. UV (MeOH): 312 (23900). ^{1}H-NMR ((D$_6$)DMSO): 2.22 (*s*, CH$_3$C); 2.29 (*m*, H$_b$–C(2′)); 2.85 (*m*, H$_a$–C(2′)); 3.14 (*s*, (CH$_3$)$_2$N); 3.42 (*m*, H–C(5′)); 3.82 (*m*, H–C(4′)); 4.45 (*m*, H–C(3′)); 4.79 (*dd*, *J* = 5.8, OH–C(5′)); 5.28 (*d*, *J* = 4.5, OH–C(3′)); 6.61 (*t*, *J* = 6.5, H–C(1′)); 8.07 (*s*, H–C(3)); 8.46 (*s*, H–C(6)). Anal. calc. for $C_{14}H_{20}N_6O_3$: C 52.49, H 6.29, N 26.23; found: C 52.53, H 6.28, N 26.18.

*4-(Benzoylamino)-1-[2′-deoxy-5′-*O*-(dimethoxytrityl)-β-*D-erythro-*pentofuranosyl]-1*H-*pyrazolo[3,4-*d*]pyrimidine* (**4c**). To a soln. of **4b** (600 mg, 1.68 mmol) in abs. pyridine (10 ml), a soln. of 4-(dimethylamino)pyridine (108 mg, 0.9 mmol) and 4,4′-dimethoxytrityl chloride (1.1 g, 3.2 mmol) in dioxane (5 ml) was added and stirred for 3 h at r.t. The reaction was monitored by TLC (silica gel, *G*). After addition of 5% aq. NaHCO$_3$ soln. (50 ml), the mixture was extracted 3 times with CH$_2$Cl$_2$ (100 ml), the combined org. phase dried (Na$_2$SO$_4$), filtered, and evaporated, and the residue applied to a 15 × 3-cm silica gel *60H* column. After washing with *E*, **4c** was eluted with *F*. Isolation of the material of the main zone yielded colorless amorphous **4c** (930 mg, 84%). TLC (silica gel, *G*): R_f 0.8. UV (MeOH): 236 (34900), 275 (16800), 282 (15700). ^{1}H-NMR ((D$_6$)DMSO): 2.38 (*m*, H$_b$–C(2′)); 2.88 (*m*, H$_a$–C(2′)); 3.07 (*m*, H–C(5′)); 3.67, 3.69 (2*s*, 2 CH$_3$O); 3.98 (*m*, H–C(4′)); 4.56 (*m*, H–C(3′)); 5.37 (*d*, *J* = 5, OH–C(3′)); 6.73 (*dd*, *J* = 9, 5, H–C(1′)); 7.14–8.11 (*m*, arom. H); 8.44 (*s*, H–C(3)); 8.79 (*s*, H–C(6)); 11.68 (*s*, NH). Anal. calc. for $C_{38}H_{35}N_5O_6$: C 69.39, H 5.36, N 10.65; found: C 69.25, H 5.55, N 10.51.

*4-(Benzoylamino)-2-(2′-deoxy-β-*D-erythro-*pentofuranosyl)-2*H-*pyrazolo[3,4-*d*]pyrimidine* (**5b**) was prepared as described for **4b**, except that **3** (500 mg, 2 mmol) in pyridine (10 ml), Me$_3$SiCl (2.6 ml, 20 mmol), and benzoyl chloride (285 µl, 2.4 mmol) were used. Compd. **5b** crystallized from H$_2$O (30 ml) in colorless needles (610 mg, 85%). TLC (silica gel, *H*): R_f 0.41. UV (MeOH): 246 (15450), 277 (13300), 315 (9550). M.p. 205°. ^{1}H-NMR ((D$_6$)DMSO): 2.43 (*m*, H$_b$–C(2′)); 2.65 (*m*, H$_a$–C(2′)); 3.58 (*m*, H–C(5′)); 3.93 (*m*, H–C(4′)); 4.45 (*m*, H–C(3′)); 4.92 (*t*, *J* = 5.5, OH–C(5′)); 5.36 (*d*, *J* = 4.4, OH–C(3′)); 6.46 (*dd*, *J* = 6.5, H–C(1′)); 7.52–8.13 (arom. H); 8.61 (*s*, H–C(6)); 8.98 (*s*, H–C(3)[3])). Anal. calc. for $C_{17}H_{17}N_5O_4$: C 57.46, H 4.82, N 19.71; found: C 57.40, H 4.85, N 20.01.

*2-(2′-Deoxy-β-*D-erythro-*pentofuranosyl)-4-{[1-(dimethylamino)ethylidene]amino}-2*H-*pyrazolo[3,4-*d*]pyrimidine* (**7**) was prepared as described for **6b** by using **3** (300 mg, 1.2 mmol) and *N,N*-dimethylacetamide dimethyl acetal (0.5 ml, 3 mmol): colorless amorphous **7** (230 mg, 60%). TLC (silica gel, *C*): R_f 0.6. UV (MeOH): 328 (20900). ^{1}H-NMR ((D$_6$)DMSO): 2.23 (*s*, CH$_3$–C); 2.36 (*m*, H$_b$–C(2′)); 2.63 (*m*, H$_a$–C(2′)); 3.14 (*s*, (CH$_3$)$_2$N); 3.53 (*m*, H–C(5′)); 3.90 (*m*, H–C(4′)); 4.42 (*m*, H–C(3′)); 4.98 (*t*, *J* = 5.5, OH–C(5′)); 5.32 (*d*, *J* = 4.3, OH–C(3′)); 6.31 (*dd*, *J* = 6, H–C(1′)); 8.42 (*s*, H–C(6)); 8.67 (*s*, H–C(3)). Anal. calc. for $C_{14}H_{20}N_6O_3$: C 52.49, H 6.29, N 26.23; found: C 52.61, H 6.29, N 26.44.

*4-(Benzoylamino)-2-[2′-deoxy-5′-*O*-(dimethoxytrityl)-β-*D-erythro-*pentofuranosyl]-2*H-*pyrazolo[3,4-*d*]pyrimidine* (**5c**) was prepared as described for **4c**, except that **5b** (500 mg, 1.4 mmol), 4-(dimethylamino)pyridine (90 mg, 0.73 mmol), 4,4′-dimethoxytrityl chloride (900 mg, 2.7 mmol), and anh. pyridine (15 ml) were used. The reaction was monitored by TLC (silica gel, *I*). FC (*I*) on a 15 × 3-cm silica gel *60H* column yielded colorless amorphous **5c** (730 mg, 79%). TLC (silica gel, *F*): R_f 0.15. UV (MeOH): 318 (9750), 277 (14600), 236 (29500). ^{1}H-NMR ((D$_6$)DMSO): 2.45 (*m*, H$_b$–C(2′)); 2.77 (*m*, H$_a$–C(2′)); 3.14 (*m*, H–C(5′)); 3.64, 3.66 (2*s*, 2 CH$_3$O); 4.05 (*m*, H–C(4′)); 4.52 (*m*, H–C(3′)); 5.43 (*d*, *J* = 4.9, OH–C(3′)); 6.52 (*m*, H–C(1′)); 6.69–8.09 (arom. H); 8.64 (*s*, H–C(6)); 8.97 (*s*, H–C(3)). Anal. calc. for $C_{38}H_{35}N_5O_6$: C 69.39, H 5.36, N 10.65; found: C 69.37, H 5.47, N 10.58.

*4-(Benzoylamino)-1-[2′-deoxy-5′-*O*-(dimethoxytrityl)-β-*D-erythro-*pentofuranosyl]-1*H-*pyrazolo[3,4-*d*]pyrimidine 3′-[Methyl* N,N-*Diisopropylphosphoramidite]* (**8a**). Compd. **4c** (800 mg, 1.2 mmol) dissolved in anh. CH$_2$Cl$_2$ (5 ml) was preflushed with Ar. Chloro(diisopropylamino)methoxyphosphine (240 µl, 1.2 mmol) and (i-Pr)$_2$EtN (615 µl, 3.6 mmol) were added by syringe, and the mixture was kept under Ar (r.t.). After 1 h, 5% aq. NaHCO$_3$ soln. (50 ml) was added and the soln. extracted 3 times with CH$_2$Cl$_2$. The org. layer was dried (Na$_2$SO$_4$) and evaporated and the residue purified by FC (*K*) on a 10 × 2-cm silica gel *60H* column yielding a colorless foam **8a** (810 mg, 83%). TLC (silica gel, *K*): R_f 0.88. ^{31}P-NMR (CDCl$_3$): 149.68.

*4-(Benzoylamino)-1-(2′-deoxy-5′-*O*-(dimethoxytrityl)-β-*D-erythro-*pentofuranosyl)-1*H-*pyrazolo[3,4-*d*]pyrimidine 3′-[(2-Cyanoethyl)* N,N-*Diisopropylphosphoramidite]* (**8b**). To a soln. of **4c** (400 mg, 0.6 mmol) in dry

[3]) Unambiguously assigned by NOE difference spectroscopy.

CH_2Cl_2 (5 ml) under N_2, $(i\text{-}Pr)_2EtN$ (350 µl, 1.8 mmol) was added under stirring at r.t., followed by chloro(2-cyanoethoxy)(diisopropylamino)phosphine (143 mg, 0.6 mmol). After 30 min, 5% aq. $NaHCO_3$ soln. (20 ml) was added and the soln. extracted 3 times with CH_2Cl_2. The org. layer was dried (Na_2SO_4) and evaporated and the residue purified by FC (silica gel *60H*, *L*, column 10 × 2 cm), yielding **8b** as a colorless amorphous foam (380 mg, 73%). TLC (silica gel, *L*): R_f 0.85. ^{31}P-NMR ($CDCl_3$): 146.93, 147.11.

*4-(Benzoylamino)-2-[2'-deoxy-5'-O-(dimethoxytrityl)-β-*D*-erythro-pentofuranosyl]-2*H*-pyrazolo[3,4-d]pyrimidine 3'-[Methyl* N,N*-Diisopropylphosphoramidite]* (**9**) was prepared as described for **8a**. Compd. **5c** (400 mg, 0.6 mmol) reacted with chloro(diisopropylamino)methoxyphosphine (120 µl, 0.6 mmol) in the presence of $(i\text{-}Pr)_2EtN$ (310 µl, 1.8 mmol): colorless, amorphous **9** (380 mg, 77%). TLC (silica gel, *L*): R_f 0.75. ^{31}P-NMR ($CDCl_3$): 147.56, 147.83.

Solid-Phase Synthesis of the Oligomers **10**–**22**. The synthesis of the oligonucleotides was performed on a 1-µmol scale using the methyl phosphoramidites of $[(MeO)_2Tr]T_d$, $[(MeO)_2Tr]bz^6A_d$, $[(MeO)_2Tr]ib^2G_d$,

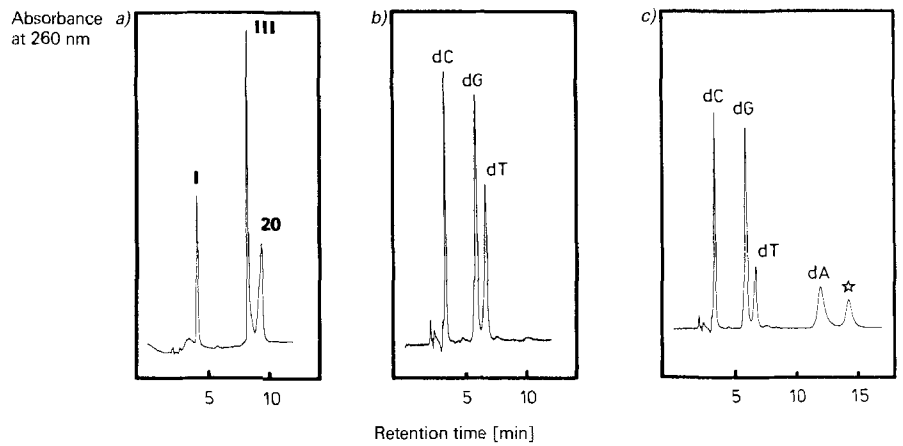

Fig. 4. *HPLC profiles obtained from the hydrolysis of the oligonucleotide d(C-T-G-G-A-T-C-C-c^{7}z^{8}A-G)* (**20**) *with the endodeoxyribonuclease Sau 3A*. Conditions as described in *Fig. 2*; d(C-T-G) (**I**), d(pG-A-T-C-C-c^{7}z^{8}A-G) (**II**), and c^{7}z^{8}A$_d$ (**2**) ☆.

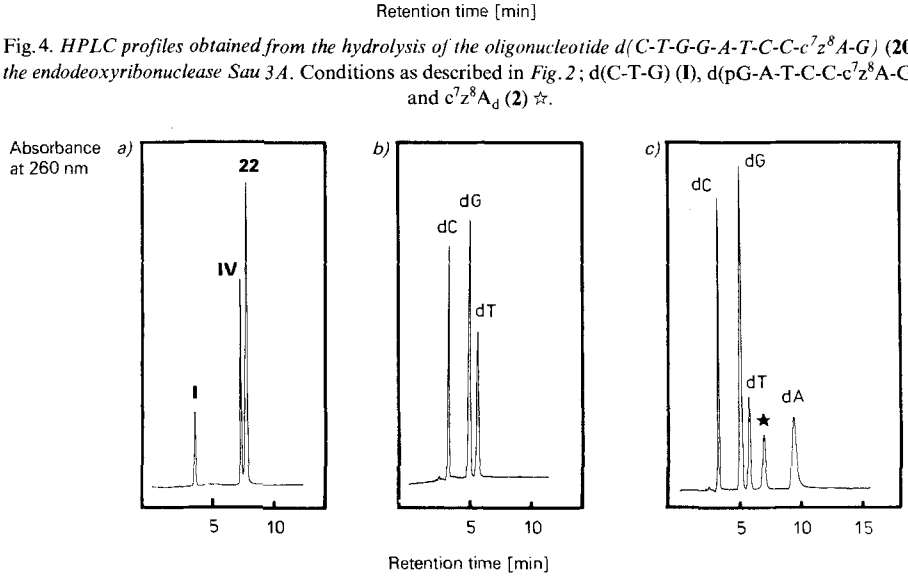

Fig. 5. *HPLC profiles obtained from the hydrolysis of the oligonucleotide d(C-T-G-G-A-T-C-C-c^{7}z^{8}A'-G)*^{1}) (**22**) *with the endodeoxyribonuclease Sau 3A*. Conditions as described in *Fig. 2*; d(C-T-G) (**I**), d(pG-A-T-C-C-c^{7}z^{8}A'-G)^1) (**IV**), and c^{7}z^{8}A'$_d$ (**3**) ★^{1}).

$[(MeO)_2Tr]bz^4C_d$, as well as **8a** or **9**. The synthesis of **10–22** followed the user manual of the DNA synthesizer for methyl phosphoramidites [18]. The oligomers were recovered from the synthesizer as the 5′-dimethoxytritylated derivatives. After their treatment with conc. NH_4OH for 16 h at 60°, the 5′-dimethoxytritylated oligomers were purified by HPLC on *RP-18* columns (250 × 4 mm, 7 μm) using solvent *I*. Detritylation with 80% AcOH afforded **10–22** which were purified by HPLC (*RP-18* column, 250 × 4 mm, 7 μm, solvent *II*). The oligomers were desalted on a 25 × 4-mm HPLC cartridge (*RP-18*, silica gel). Inorg. material was eluted with H_2O (10 ml), while the oligomers were eluted with $MeOH/H_2O$ 3:2 (5 ml). The oligomers were lyophilized on a *Speed-Vac* evaporator to give colorless foams (*ca.* 0.3 μmol, 30%). They were dissolved in H_2O (1 ml) and stored frozen at −20°.

Enzymatic Hydrolysis of the Oligomers **10–22**. The oligomer (0.5 A_{260} units) was dissolved in 0.1M *Tris*-HCl buffer (pH 8.5; 200 μl) and treated with snake-venom phosphodiesterase (3 μg) at 25° for 45 min and alkaline phosphatase (2 μg) for 30 min at 25°. The mixture was analyzed on reverse-phase HPLC (*RP-18* column, 4 × 250 mm, solvent *III*). Quantification of the material was made at 260 nm on the basis of the peak areas which were divided by the extinction coefficients of the nucleoside constituents (ε_{260}: dA, 15400; dC, 7300; dG, 11300; dT, 8800; **2**, 9000; **3**, 7100). See *Figs. 2, 4,* and *5*.

Phosphodiester Hydrolysis of the Oligomers **17–22**. The Oligomers **17–22** (0.25 A_{260} units, each) were dissolved in 6 mM *Tris*-HCl buffer (pH 7.5) containing 50 mM NaCl and 6 mM $MgCl_2$ (160 μl) and were treated with the endodeoxyribonuclease Sau 3A (3 μl (12 units) of enzyme suspension in buffer containing 20 mM *Tris*-HCl, pH 7.5, 50 mM NaCl, 0.1 mM EDTA, 5 mM EtSH/glycerol 1:1). The soln. was stored at 25°, 15-μl samples were taken at different intervals of time and analyzed on reverse-phase HPLC (*RP 18,* 250 × 4 mm column, solvent *II*; see *Fig. 3*). The hydrolysis products were collected, lyophilized, and analyzed after tandem hydrolysis with snake-venom phosphodiesterase and alkaline phosphatase, as described in the previous section.

REFERENCES

[1] W. Saenger, in 'Principles of Nucleic Acid Structures', Ed. C. R. Cantor, Springer Verlag, New York, 1984, pp. 253.
[2] A. Rich, A. Nordheim, A. H.-J. Wang, *Ann. Rev. Biochem.* **1984,** *53,* 791.
[3] H.-M. Wu, D. M. Crothers, *Nature (London)* **1984,** *308,* 509.
[4] F. Seela, H. Steker, *Helv. Chim. Acta* **1985,** *68,* 563.
[5] J. S. Sussenbach, C. H. Monfoort, R. Schiphof, E. E. Stobberingh, *Nucleic Acids Res.* **1976,** *3,* 3193.
[6] B. S. Sproat, M. J. Gait, in 'Oligonucleotide Synthesis, A Practical Approach', Ed. M. J. Gait, IRL-Press, 1984, pp. 83.
[7] F. Seela, B. Westermann, U. Bindig, *J. Chem. Soc., Perkin. Trans. 1* **1988,** 697.
[8] R. K. Robins, *J. Am. Chem. Soc.* **1956,** *78,* 784.
[9] M. Hoffer, *Chem. Ber.* **1960,** *93,* 2777.
[10] G. S. Ti, B. L. Gaffney, R. A. Jones, *J. Am. Chem. Soc.* **1982,** *104,* 1316.
[11] J. Zemlicka, J. Holy, *Collect. Czech. Chem. Commun.* **1967,** *32,* 3159.
[12] L. J. McBride, R. Kierzek, S. L. Beaucage, M. H. Caruthers, *J. Am. Chem. Soc.* **1986,** *108,* 2040.
[13] H. Berg, unpublished data.
[14] H. Schaller, G. Weimann, B. Lerch, H. G. Khorana, *J. Am. Chem. Soc.* **1963,** *85,* 3821.
[15] M. D. Matteucci, M. H. Caruthers, *J. Am. Chem. Soc.* **1981,** *103,* 3185.
[16] N. D. Sinha, J. Biernat, J. McManus, H. Köster, *Nucleic Acids Res.* **1984,** *12,* 4539.
[17] L. J. McBride, M. H. Caruthers, *Tetrahedron Lett.* **1983,** *24,* 245.
[18] Applied Biosystems, 'User Manual', edn. 1986.
[19] V. A. Bloomfield, D. M. Crothers, I. Tinoco, in 'Physical Chemistry of Nucleic Acids', Ed. J. A. Woods, Harper and Row, New York, 1974, pp. 349.
[20] W. D. Wilson, E. T. Zuo, R. L. Jones, G. L. Zon, B. R. Baumstark, *Nucleic Acids Res.* **1987,** *15,* 105.
[21] M. A. Viswamitra, Z. Shakked, P. G. Jones, G. M. Sheldrick, S. A. Salisbury, O. Kennard, *Biopolymers* **1982,** *21,* 513.
[22] A. Klug, A. Jack, M. A. Viswamitra, O. Kennard, Z. Shakked, T. A. Steitz, *J. Mol. Biol.* **1979,** *131,* 669.
[23] A. Ono, M. Sato, Y. Ohtani, T. Ueda, *Nucleic Acids Res.* **1984,** *12,* 8939.
[24] F. Seela, A. Kehne, *Biochemistry* **1987,** *26,* 2232.
[25] J. A. McClarin, C. A. Frederick, B.-C. Wang, P. Greene, H. W. Boyer, J. Grable, J. M. Rosenberg, *Science* **1986,** *234,* 1526.
[26] F. Seela, W. Herdering, A. Kehne, *Helv. Chim. Acta* **1987,** *70,* 1649.